Food Chemistry: X 15 (2022) 100408

Contents lists available at ScienceDirect

Food Chemistry: X

journal homepage: www.sciencedirect.com/journal/food-chemistry-x

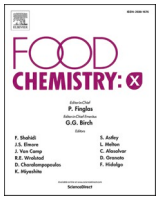

Gellan gum conjugation with soy protein *via* Maillard-driven molecular interactions and subsequent clustering lead to conjugates with tuned technological functionality

Yasaman Lavaei, Mehdi Varidi *, Majid Nooshkam

Department of Food Science and Technology, Faculty of Agriculture, Ferdowsi University of Mashhad (FUM), Mashhad, Iran

ARTICLE INFO

Keywords:
Soy protein isolate
Interfacial activity
Gellan gum
Protein-polysaccharide conjugate
Conjugation degree
Functional properties
Antioxidant activity

ABSTRACT

Soy proteins are frequently used in the food industry; however, they have rigid and compact structure with relatively poor interfacial properties and solubility. This study was therefore aimed to modify techno-functional characteristics of soy protein isolate (SPI; 0.1% w/v) by conjugating to low acyl gellan gum (LAGG; 0.1, 0.2, and 0.3% w/v), through the Maillard reaction (at 90 °C for 90 min). The SPI-LAGG conjugates were confirmed by changes in pH, glycation degree (DG; up to 48%), Fourier transform infrared spectroscopy, and sodium dodecyl sulphate polyacrylamide electrophoresis. The conjugates were then classified into three clusters of low, medium, and high DG, *via K*-means clustering method. The low DG conjugate had lower surface hydrophobicity and foaming capacity, and higher thermal stability, solubility, emulsifying properties, foam stability, and antioxidant activity compared to the other clusters. This indicated that a low DG is required to enhance the functional properties of proteins.

1. Introduction

Plant-derived proteins are considered to become the most important protein source in the future. The global challenge of preserving land and water resources due to climate change as the defining issue of our time, addressing food security as well as a shift in the consumer choices toward vegan diet or more natural products has intensified the discussion of replacing animal-based protein with plant-based ones more than the past. In this context, the global market worth of natural and sustainable food and beverages with "clean labels" is expected to reach USD 47.5 billion by 2023 (Kutzli et al., 2021).

Glycine max belongs to the *Leguminosae* family and is commonly known as soybean plant. Soy proteins are considered as an abundant by-product from soybean oil processing, which have been increasingly applied in the food industry due to their low cost, desirable functional properties, high nutritional value, and health-promoting effects, such as lowering serum cholesterol level (Ma, Chen, et al., 2020). Soy protein isolate (SPI), as an ideal protein product that contains >90% protein, consists of two main fractions glycinin (11S) and β-conglycinin (7S) based on the sedimentation coefficient, which are classified as the globular storage proteins responsible for the functional properties of SPI (Li et al., 2019). Due to the amphiphilic nature of SPI, researchers have paid more attention to its emulsification properties (Kutzli et al., 2021; Li et al., 2019). However, the rigid and compact structure of globular proteins, due to the conformational stability caused by hydrogen and disulfide bonds along with low molecular flexibility, has affected their interfacial and emulsifying properties, leading to poor functional properties of native SPI than relatively flexible proteins such as casein (Mozafarpour et al., 2019). Moreover, SPI shows poor solubility, especially at pH = 4–6, while protein solubility in aqueous media is an important prerequisite for the manifestation of desirable techno-functional properties in food systems. This also limits the protein application particularly in low viscosity products such as beverages, where gravitational separation and turbidity are undesirable (Kutzli et al., 2021). On the other hand, in order to achieve maximum shelf life, proper consumption, and consider the preferences of modern consumers, most soy products are supplied in dry forms. However, due to the general instability of proteins against thermal processing, the application of high temperatures during drying process may have adverse effects on the performance and stability of soy proteins (Boostani et al., 2017). These limitations impede the ideal technological performance and industrial applications of SPI.

There are several modification approaches to overcome these limitations. Natural modification methods have received great attentions in

* Corresponding author.
E-mail address: m.varidi@um.ac.ir (M. Varidi).

https://doi.org/10.1016/j.fochx.2022.100408
Received 24 May 2022; Received in revised form 6 July 2022; Accepted 4 August 2022
Available online 8 August 2022

recent years. Proteins glycation *via* carbohydrates is one of the natural proteins modification methods that occurs at the early stages of the Maillard reaction through covalent attachment between the free amino groups of proteins (especially ε-amino group of lysine residues) and the terminal reducing carbonyl groups of sugars during the heat treatment (Nooshkam & Varidi, 2020a). The Maillard reaction irreversibly changes protein and carbohydrate structures in comparison to other non-covalent reaction approaches, and it is known as a cost-effective, facile, and safe method, which would be done spontaneously without any requirement for additional chemical reagents (Naik et al., 2021). The Maillard conjugation under mild and controlled conditions, in most cases, ameliorates protein functionalities such as solubility, emulsifying activity, thermal stability, and antioxidant activity (Nasrollahzadeh et al., 2017; Nooshkam & Madadlou, 2016a, 2016b; Nooshkam & Varidi, 2020b). However, it seems necessary to prevent the Maillard reaction progression to the advanced stages in order to limit the formation of uncertain and harmful components, which could lead to various diseases such as diabetes and Alzheimer's (Ma, Hou, et al., 2020). The weak reducibility and strong steric hindrance of polysaccharides compared to mono- and oligosaccharides lead to more restriction in the extent of the Maillard reaction, brown color development, and protein polymerization (Nooshkam & Varidi, 2020a).

Gellan gum (GG) is a biodegradable and anionic microbial polysaccharide with a tetrasaccharide repeating unit (two β-(1 → 3)-D-glucose, one β-(1 → 4)-D-glucuronic acid, and one α-(1 → 4)-L-rhamnose) (Chen et al., 2020; Nooshkam & Varidi, 2021). It is widely used in the food industry due to its gelation, resistance to heat and pH at extremely low concentrations (Kazemi-Taskooh & Varidi, 2021), and potential to stabilize oil-in-water emulsions through electro-steric mechanism (Nooshkam & Varidi, 2020b).

As mentioned, it is mandatory to stop the conjugation reaction in the early stage to prepare protein-polysaccharide conjugates with enhanced techno-functional properties and minimum level of brown polymers and advanced glycation end-products (Nooshkam & Varidi, 2020a). Glycation degree (DG) is one of the most important physicochemical properties of Maillard reaction products (MRPs), which is frequently used to evaluate the extent of the Maillard reaction. The DG has a major effect on the functional and biological properties of conjugates (Martinez-Alvarenga et al., 2014; Nooshkam & Varidi, 2020b). This study was therefore aimed to use *K*-means clustering approach to classify the SPI-low acyl GG (SPI-LAGG) conjugates into three clusters of low, medium, and high DG, in order to investigate the effect of DG on the structural, techno-functional, and antioxidant properties of SPI-LAGG conjugates.

2. Materials and methods

2.1. Materials

SPI (90% protein content) and LAGG (≥85% gellan content; 200–300 kDa) were supplied from Yuwang Co. (China) and Amstel Products BV Co. (The Netherlands), respectively. Other chemicals were of analytical reagent grade and obtained from Sigma-Aldrich Co. (St Louis, MO, USA) and Merck Co. (Darmstadt, Germany).

2.2. Preparation of SPI-LAGG conjugates

LAGG (0.1, 0.2, and 0.3% w/v) and SPI (0.1% w/v) were dispersed in 10 mM phosphate buffer solution (pH 7) and stirred for 3 h at 25 °C. After complete hydration (12 h, 4 °C), the SPI-LAGG solution was heated in a water-bath at 90 °C for 30, 60, and 90 min. The solution was cooled down to 25 °C to terminate the reaction, and the prepared samples were stored at 4 °C for following experiments. The non-heated SPI-LAGG mixtures (SPI-LAGG-0) and native SPI were taken as controls.

2.3. Conjugate characterization

2.3.1. pH changes

The pH value of the samples before and after the heating process was recorded at room temperature by a pH meter (827 pH Lab, Metrohm, Switzerland).

2.3.2. Absorbance at 294 nm and 420 nm

The amounts of Maillard reaction intermediate and final products were determined by measurement of the absorbance of SPI-LAGG conjugates at 294 nm and 420 nm, respectively, against the non-glycated SPI-LAGG pairs (Nooshkam & Madadlou, 2016a).

2.3.3. Free amino groups concentration

The DG of SPI-LAGG conjugates was calculated by evaluating the free amino groups concentration of conjugates compared with that of unconjugated samples, through the *ortho*-phthaldialdehyde (OPA) colorimetric assay, according to our recent report (Nooshkam & Varidi, 2020b):

$$DG\ (\%) = \left(1 - \frac{free\ amino\ groups\ (mg/mL)\ in\ glycated\ samples}{free\ amino\ groups\ (mg/mL) in\ non-glycated\ sample}\right) \times 100 \quad (1)$$

2.3.4. Electrophoretic pattern and Fourier transform infrared (FTIR) spectroscopy analysis

The electrophoretic mobility and structural changes of the conjugates were evaluated based on a previous procedure reported by Nooshkam and Varidi (2020b).

2.3.5. Differential scanning calorimetric (DSC) analysis

The thermogram patterns of freeze-dried SPI-LAGG conjugates were investigated using a DSC device (DSC100-L, China). The samples (8 mg) were hermetically sealed in aluminum pans and heated at a temperature range of 25–150 °C with a heating rate of 10 °C/min. In all curves, V and ˆ represent endothermic and exothermic peaks, respectively.

2.3.6. Surface hydrophobicity (H_0) analysis

The H_0 values of SPI, SPI-LAGG conjugates, and their physical mixtures were measured according to the 8-anilinonaphtalene-1-sulfonic acid (ANS) method described by Feyzi et al. (2018).

2.3.7. Protein solubility

Solubility of SPI, SPI-LAGG mixtures, and SPI-LAGG conjugates were examined at pHs 4.5 and 7, based on a method described by Nasrollahzadeh et al. (2017) with slight modifications. The liquid samples were centrifuged (7000 × g, 15 min, room temperature) and the protein content of the supernatant was measured using the Biuret method as below:

$$Solubility\ (\%) = \frac{Ps\ (mg/\ mL)}{Pi\ (mg/mL)} \times 100 \quad (2)$$

where, Ps and Pi are the protein contents in the supernatant and initial solution, respectively.

2.3.8. Viscosity

The rheological properties of the samples, with protein content of 1 mg mL^{-1}, were evaluated by a Brookfield viscometer (LVDV III-ULTRA, Brookfield, USA) at 25 °C, by LV1 and LV2 spindles at shear rate range of 0.01–100 s^{-1}. The Power-law equation was the best model to fit the shear rate and shear stress data, using SlideWrite Plus Software (version 7.01):

$$\tau = K\gamma^n \quad (3)$$

where, τ indicates the shear stress (Pa), γ stands for the shear rate

(s^{-1}), K represents the consistency coefficient (Pa s^n), and n displays the flow behavior index (dimensionless). In addition, the apparent viscosity of all systems was measured at 50 s^{-1}.

2.3.9. Surface and interfacial tension

A tensiometer (K100, Kruss, Germany) was used to determine the surface (mN m^{-1}) and interfacial (mN m^{-1}) tensions of the samples according to the Du Nouy ring method, according to the methods of Mozafarpour et al. (2019).

2.3.10. Emulsifying properties

The emulsifying properties of the samples were measured according to Pearce and Kinsella (1978) procedure, with some modifications. The emulsions were prepared by homogenization of 25 mL sample solution (1 mg mL^{-1} protein; pH 7) with 8.3 mL sunflower oil at 10,000 rpm for 1 min using an Ultra-Turrax T25 homogenizer (IKA-Labortechnik, Staufen, Germany). Next, 100 μL of obtained emulsion was pipetted from the bottom of the test tube (at times zero and 30 min), and immediately diluted with 5 mL of 0.1% w/v SDS. Emulsifying properties of the samples were measured from the absorbance of the diluted emulsion at 500 nm, according to the following equations:

$$\text{Emulsifying activity index } (EAI;\ m^2/g) = \left(\frac{2 \times 2.30 \times A0 \times DF}{C \times L \times (1-\theta) \times 10000}\right) \quad (4)$$

$$\text{Emulsion stability index } (ESI;\ \text{min}) = \left(\frac{A0 \times 30}{A0 - A30}\right) \quad (5)$$

where, A_0 and A_{30} are the absorbances of the diluted emulsion at 0 min and 30 min after emulsion formation, respectively. C indicates the initial protein content (mg mL^{-1}), DF represents the dilution factor (50), θ displays the oil fraction (0.25), and L referred to the optical path length (0.01 m).

2.3.11. Droplet size

The emulsions were diluted 100-fold using 10 mM sodium phosphate buffer (pH 7) and the measurements were obtained by a dynamic light scattering analyzer (Cordouan, Vasco3, France). The results were expressed as the Z-average size and polydispersity index (PDI).

2.3.12. ζ-potential

A Zeta potential Analyzer (Zeta compact, CAD instrumentation, France) was utilized to estimate the surface charge of emulsion droplets (Caballero & Davidov-Pardo, 2021).

2.3.13. Foaming properties

Foaming properties of the samples (1 mg mL^{-1} protein) were determined according to Feyzi et al. (2018) procedure, with some changes. The non-conjugated and conjugated samples (25 mL) were whipped vigorously for 1 min by an Ultra-Turrax T25 at 10,000 rpm. The foam capacity (FC) percentage was determined as below:

$$\text{FC } (\%) = \left(\frac{V1 - V0}{V0}\right) \times 100 \quad (6)$$

where V_1 is the total volume (mL) of the solution and foam after whipping, and V_0 is the solution volume (mL) before whipping.

Foam stability (FS) of the samples was considered as the foam volume remaining after 30 min at ambient temperature, and was calculated as follows:

$$FS(\%) = \left(\frac{V2 - V0}{V1 - V0}\right) \times 100 \quad (7)$$

where V_2 is the total volume of the solution and foam after 30 min.

2.3.14. Antioxidant activity

Reducing power and DPPH-free radical scavenging (DPPH-RS) activity of conjugates were determined according to procedures reported by Nooshkam, Falah, et al. (2019) and Lertittikul et al. (2007).

2.4. Statistical analysis

A completely randomized design in factorial arrangement with two factors of heating time (4 levels) and LAGG content (3 levels) was performed and the results of the Maillard reaction progression were analyzed by Minitab software (version 16). The treatments were then classified into three clusters in the term of DG (i.e., low, medium, and high DG) using *K*-means clustering method, by SPSS software (version 26). The results of the last part were analyzed according to the first part. The differences between means were determined by the Tukey test at 95% confident level. The experiments were repeated three times.

3. Results and discussion

3.1. Maillard reaction progression

3.1.1. Changes in pH

The pH value decreased markedly in all the SPI-LAGG mixtures after conjugation reaction (Fig. 1a). The SPI-LAGG mixtures underwent a significant pH decrease (ca. 7.000 to 6.902) as the reaction prolonged to 90 min, mainly due to the consumption of free amino groups and the formation of acidic compounds (Consoli et al., 2018). The pH value of the systems was firstly decreased significantly as the gellan level rose from 0.1 to 0.2%, and the parameter was then increased in the systems containing 0.3% gellan polysaccharide ($p < 0.05$); the SPI-0.1LAGG, SPI-0.2LAGG, and SPI-0.3LAGG systems indicated pH values of 6.964, 6.903, and 6.936, respectively (Fig. 1a). Indeed, the SPI-0.1LAGG system had the highest DG compared to the other counterparts (see section 3.1.3), and the synthesized conjugates with high molecular weight (HMW) could likely restrict the conversion of Amadori or Heyns products to acidic compounds through steric hindrance (Ma, Hou, et al., 2020). The lower pH of SPI-0.2LAGG system in comparison to the other pairs might be ascribed to its higher content of reactive carbonyl groups, thereby increasing the interaction between SPI and LAGG, and causing a further reduction in the pH value of the system. However, higher gellan concentration (i.e., 0.3%) increased the system's viscosity, and the molecular motion and interaction between gellan and protein molecules could be subsequently decreased (Nooshkam, Falah, et al., 2019), leading to a lower neutral-to-acidic pH shift.

3.1.2. Intermediate and final products

The Abs 294 nm decreased as the heating time increased; whilst, the parameter increased with increasing gellan concentration (Fig. 1b). Indeed, the highest and lowest Abs 294 nm were observed in SPI-0.3LAGG-30 and SPI-0.1LAGG-90 systems, respectively. Intermediate products were largely generated during the initial period of the reaction (i.e., 30 min) and further heating times led to a lower Abs 294 nm, likely as a consequence of acidic compounds formation (Fig. 1a) and the consumption a large number of amino groups during the first part of the heating reaction (see section 3.1.3). The system is therefore shifted to more acidic conditions as the reaction time increased to 90 min, and the formation of intermediate compounds could be consequently decreased at low pH value of the reaction system.

The final products of the Maillard reaction experienced a similar trend (Fig. 1c). The higher heating times resulted in a conjugate with smaller Abs 420 nm. This could be likely ascribed to brown pigments' degradation at extended heating times (Nooshkam & Varidi, 2020b). It is also noteworthy that the Abs 294 and 420 nm of the conjugates increased as a function of gellan concentration. Accordingly, the highest and lowest absorption values were found in 0.3%LAGG and 0.1%LAGG systems, respectively. The SPI-0.3LAGG systems with the lowest DG and

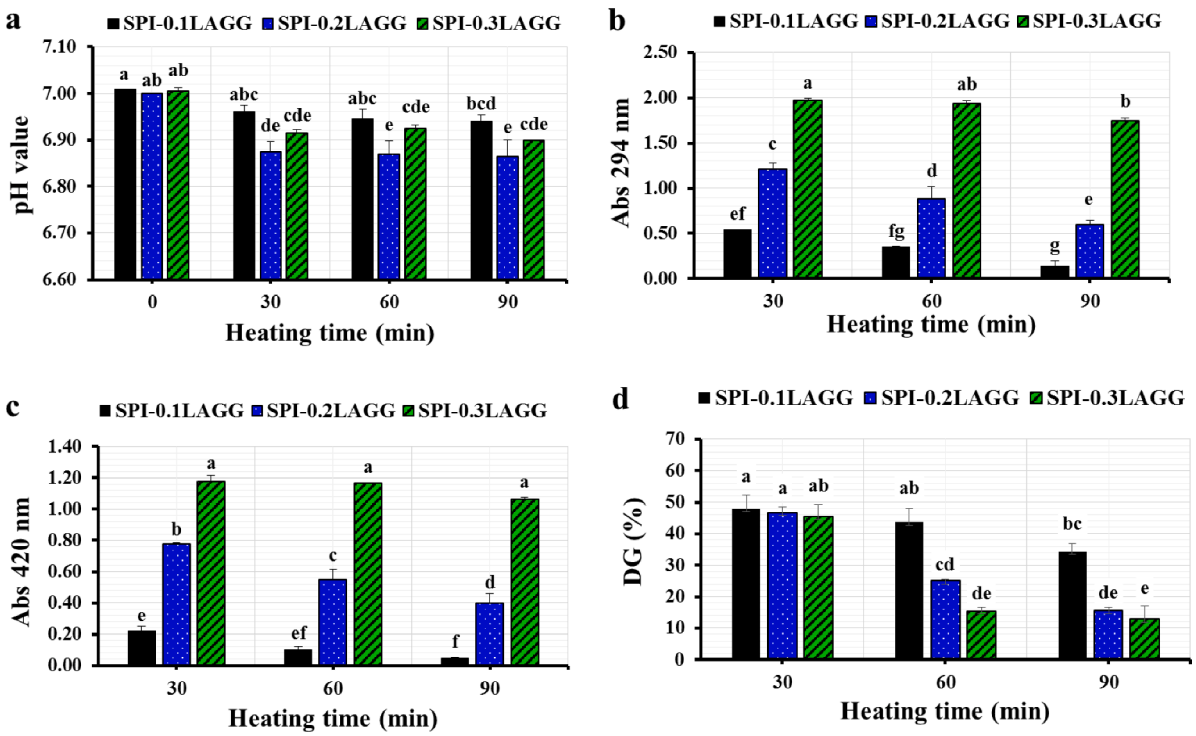

Fig. 1. Changes in pH value (a), Abs 294 nm (b), Abs 420 nm (c), and glycation degree (d) of soy protein isolate-low acyl gellan gum (SPI-LAGG) solution as a function of heating time.

consequently the formation of low molecular weight conjugates could participate more rapidly in the Maillard reaction progression to convert primary products into intermediate and advanced ones than other system counterparts. In general, the higher Abs 294 nm values compared to the Abs 420 nm ones demonstrate that the non-enzymatic browning reaction between LAGG and SPI is most probably dominated at the early stage.

3.1.3. Glycation degree

The DG of glycated systems decreased markedly as the concentration of LAGG increased, and the maximum and minimum DG values were accounted for SPI-0.1LAGG (41.99%) and SPI-0.3LAGG (24.63%) systems, respectively (Fig. 1d). The higher system viscosity as a result of higher LAGG concentration could reduce the molecular motion and the interaction between SPI and LAGG, likely resulting in a lower DG (Nooshkam, Falah, et al., 2019). The complicated structures along with higher steric hindrance as a consequence of LAGG level increment could lead to a decreased DG value, as well (Ma, Chen, et al., 2020). On the other hand, the DG decreased generally from 46.71% to 20.95% as the reaction time increased from 30 to 90 min. This may be ascribed to the greater level of carbonyl groups during the first heating period of the reaction, which could lead to the higher reactivity of the system. Subsequently, further heating time along with more protein denaturation could release higher amino groups rather than Maillard reaction progression (Nooshkam & Varidi, 2020b). The highest and lowest extent of DG were observed in SPI-0.1LAGG-30 and SPI-0.3LAGG-90 systems, respectively.

3.1.4. Electrophoretic pattern

Lane 1 shows pure protein and three lanes 2, 6, and 10 show SPI-0.1LAGG-0, SPI-0.2LAGG-0, and SPI-0.3LAGG-0 mixtures, respectively, which had similar patterns as the native SPI, indicating that covalent bands were not likely formed between SPI and LAGG in the non-heated mixture systems (Fig. 2a). Glycinin is a heterogeneous oligomeric protein with 6 acidic polypeptide chains (AS; 35–45 kDa) and 6 basic polypeptide chains (BS; 18–20 kDa), which are linked together by a disulfide bond (Petruccelli & Anon, 1995). β-conglycinin, a heterogeneous glycoprotein, contains α' (72 kDa), α (68 kDa), and β (52 kDa) subunits (Denavi et al., 2009). These characteristic bands of SPI can be seen clearly in lane 1. Generally, the intensity of SPI bands was decreased in the heated SPI-LAGG systems (lanes 3–5, 7–9, and 11–13), indicating that SPI contributed to the Maillard reaction. Moreover, the appearance of more intense bands at the top of injection wells of SPI-LAGG conjugates might represent the synthesis of HMW conjugates during the Maillard reaction (Nooshkam & Varidi, 2020b). Indeed, covalent attachment of HMW LAGG to SPI has resulted in the formation of heavy conjugates which most of them were not able to migrate into the resolving gel.

3.2. K-means clustering

The classification of protein-polysaccharide Maillard-based conjugates can help predict their technofunctional and biological functions as a first step in their use as food ingredients. This objective could be achieved by cluster analysis within the framework of pattern recognition theory. In this method, partial membership could be shared by two or more classes, while a product's membership in traditional grouping methods is only class specific. The clustering method is used to find a matching set of samples within a known dataset. The *K*-means clustering technique classifies a dataset into discrete groups with *K*-numbers by finding patterns inherent to the set. The technique is completed by the following steps (Nasrollahzadeh et al., 2017; Nooshkam, Falah, et al., 2019):

- Determine *K*-random centroids for each cluster,
- Match the data from each sample to the nearest centroid,
- Form an initial cluster through first-step completion,
- Estimate new centroids by averaging the data in each cluster,
- Reassign sample data to the nearest new centroids,
- Create a loop by changing the cluster of centroids several times until that the centroids are no longer modified.

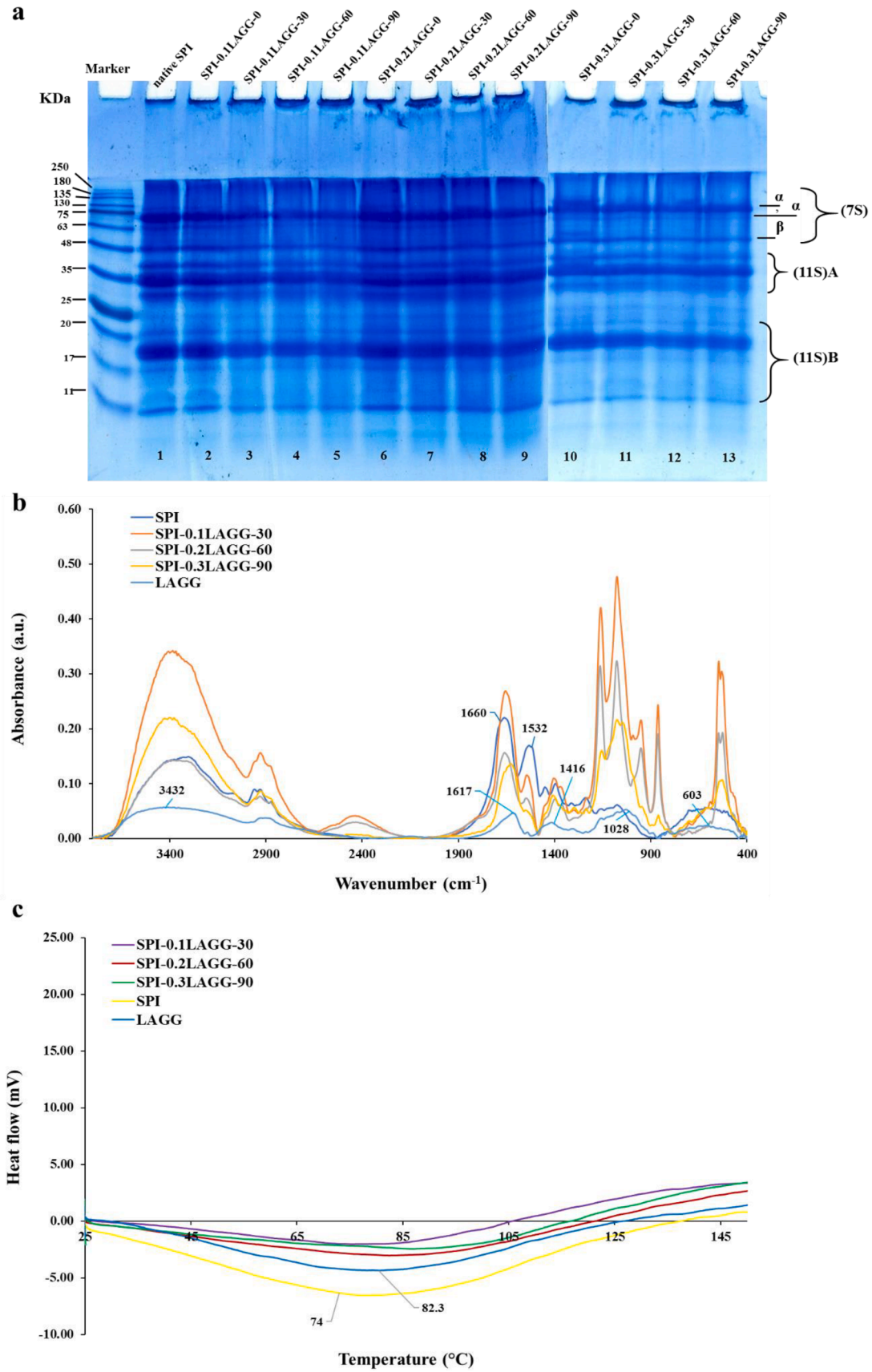

Fig. 2. SDS-PAGE patterns (a), FTIR spectra (b), and DSC thermogram (c) of soy protein isolate (SPI) and soy protein isolate-low acyl gellan gum (SPI-LAGG) mixtures and conjugates.

In this way, samples with specific characteristics can be classified into *K* clusters. Accordingly, 9 treatments were classified into 3 different groups with 3 levels of DG, which are low, medium, and high DG. The clusters were chosen by considering the effects of heating time and LAGG concentration on the DG, and the significant difference between the DG of the treatments. Finally, the following treatments were selected to be evaluated for structural changes and technological functionality of the conjugates:

- *Low DG*; SPI-0.3LAGG-90
- *Medium DG*; SPI-0.2LAGG-60
- *High DG*; SPI-0.1LAGG-30

Moreover, the corresponding non-heated SPI-LAGG pairs and SPI were considered as controls. This selective mode made it possible to select treatments with a maximum difference so that the effect of each treatment on the conjugated protein is clearly studied.

3.3. Structural changes

3.3.1. FTIR

The FTIR spectra of SPI, LAGG, and SPI-LAGG conjugates (SPI-0.1LAGG-30, SPI-0.2LAGG-60, and SPI-0.3LAGG-90), are depicted in Fig. 2b. The characteristic peaks of amides I, II, and III in the SPI spectrum were observed at 1660, 1532, and 1450–1200 cm^{-1}, respectively (Boostani et al., 2017). The characteristic bands of LAGG appeared at around 600 cm^{-1} (long chains in the biopolymer), 1028 cm^{-1} (C—O stretching vibrations), 1416 cm^{-1} (CH_3 and CH_2 bending vibrations), 1617 cm^{-1} (C═O stretching vibration), 2905 cm^{-1} (C—H stretching vibration), and 3432 cm^{-1} (hydroxyl groups) (Kazemi-Taskooh & Varidi, 2021). The covalent binding of LAGG to SPI *via* the Maillard reaction could lead to some remarkable changes in the mid-IR spectrum of the proteins.

The peaks at 1660 cm^{-1} (amide I) and 1532 cm^{-1} (amide II) were shifted up to 1625 cm^{-1} and 1551 cm^{-1}, respectively, after the Maillard reaction. This could be probably due to the occurrence of new interactions in the SPI-LAGG systems as a result of conjugation reaction (Nooshkam & Madadlou, 2016a). SPI-0.1LAGG system with the highest DG and consequently the most content of Amadori compounds with the characteristic C═O bonds, had the highest adsorption intensity in this region (Boostani et al., 2017). In contrast, the Maillard reaction progression and conversion of Amadori or Heyns products to other compounds in SPI-0.2LAGG-60 and SPI-0.3LAGG-90 systems were significantly higher than SPI-0.1LAGG-30 system (Fig. 1), which led to a remarkable decrease in the adsorption intensity of the mentioned region, that was also confirmed by the results of Abs 294 and 420 nm. As can be observed in Fig. 2b, the absorption bands in the amide II and amide III region decreased sharply after conjugation, suggesting that SPI might have participated in the Maillard conjugation and lost certain numbers of NH_2 groups. The new band at about 860 cm^{-1} in the conjugates spectra could be attributed to the C—H pyrrole bending (Abellán et al., 2013).

The peaks appeared in the wavenumber region from 800 to 1200 cm^{-1} are commonly considered as the "fingerprint region" which are related to C—C and C—O stretching vibrations and C—H bending (Mao et al., 2018). The intensity of corresponding peaks increased dramatically in SPI-LAGG conjugates compared to SPI, suggesting that the LAGG was attached to SPI successfully (Boostani et al., 2017). As the DG increased, the absorption intensity of these peaks rose markedly.

3.3.2. DSC

The thermogram patterns of SPI, LAGG, and SPI-LAGG conjugates (SPI-0.1LAGG-30, SPI-0.2LAGG-60, and SPI-0.3LAGG-90), are illustrated in Fig. 2c. Thermal denaturation of native SPI was characterized by one major peak at a maximum temperature of 74 °C, which has been related to the β-conglycinin denaturation as one of the main fractions of SPI (Namli et al., 2021).

The thermogram of pure LAGG showed an endothermic peak at a maximum temperature of 82.3 °C (Fig. 2c), relating to loss of water molecules due to gum dehydration in the temperature range of 72–99 °C (Kazemi-Taskooh & Varidi, 2021). In all SPI-LAGG conjugates, a single broad peak was observed at the temperature range studied (25 °C to 150 °C), indicating that SPI and LAGG are highly compatible (Su et al., 2010).

The maximum peak temperature (T_m) was considered as the thermal stability of the protein. There was a significant difference ($p < 0.05$) between the T_m of systems containing SPI-LAGG conjugates (Table 1). The peak temperature increased markedly as the DG decreased, and the highest and lowest T_m were observed in SPI-0.3LAGG-90 (low DG; 86.6 °C) and SPI-0.1LAGG-30 (high DG; 77.7 °C) systems, respectively. This means that the low DG conjugate presented a higher thermal stability (up to 1.11-fold) in comparison to other conjugates. Moreover, all the conjugates had higher T_m than the unheated SPI. It has been reported that covalent attachment of hydrophilic and charged polysaccharide to proteins could restrict the conformational entropy of the protein chains and stabilize the protein structure subsequently, through both steric (especially HMW polysaccharides) and electrostatic repulsions (Damodaran & Parkin, 2017). Although SPI-0.3LAGG-90 system had the lowest DG, the presence of higher content of LAGG in the reaction medium could force the protein to adopt a more compact and steady-state structure compared to the other conjugate counterparts, through macromolecular crowding effect (Álvarez et al., 2012). It is worth mentioning that the denaturation enthalpy of SPI-LAGG conjugates decreased markedly than the native SPI, which can be attributed to the exothermic nature of the conjugation reaction (Nooshkam et al., 2020).

3.3.3. Surface hydrophobicity

Conjugation of SPI-LAGG mixture systems led to a marked increase in the H_0 value on average from 2171 to 2799 ($p < 0.05$) (Fig. 3). The H_0 decreased markedly as the concentration of LAGG increased, and the highest and lowest H_0 values were found in 0.1%LAGG (~2825) and 0.3%LAGG (~2254) systems, respectively (Fig. 3). This could be attributed to the shielding effect of polysaccharide chain which hinders ANS binding to hydrophobic residues, so H_0 reduces (Zhao et al., 2020). Moreover, the highest H_0 value in SPI-0.1LAGG might be due to their higher available protein concentration than other systems, probably leading to a greater ANS fluorescence intensity (Uruakpa & Arntfield, 2006).

As can be seen in Fig. 3, the highest and lowest H_0 values were found in the SPI-0.1LAGG-30 conjugate (~3323) and SPI-0.2LAGG mixture (~1940) systems, respectively ($p < 0.05$). Moreover, the low DG conjugate had lower H_0 (up to 0.65-fold) compared to the other counterparts. Despite the fact that SPI-0.1LAGG-30 system had the highest DG, its lower T_m along with more protein denaturation extent than other conjugates could likely lead to the exposure of more hydrophobic groups and consequently a significant increase in the H_0 value (up to ~ 1.47-

Table 1
The onset (T_0) and peak temperature (T_m) and enthalpy (H) of the main peaks in thermogram of soy protein isolate (SPI), low acyl gellan gum (LAGG), and SPI-LAGG conjugates.

Samples	T_0 (°C)	T_m (°C)	H (J/g)
SPI*	53.40 ± 0.57	74.00 ± 0.85	34.06 ± 0.96
LAGG*	51.00 ± 2.55	82.30 ± 0.28	55.70 ± 2.70
SPI-0.1LAGG-30 (High DG)	55.00 ± 0.78^{b}	77.70 ± 1.10^{b}	29.73 ± 1.84^{a}
SPI-0.2LAGG-60 (Medium DG)	61.10 ± 0.78^{a}	83.20 ± 0.95^{ab}	31.61 ± 0.71^{a}
SPI-0.3LAGG-90 (Low DG)	60.50 ± 0.42^{a}	86.60 ± 1.82^{a}	20.55 ± 1.06^{b}

Means within the same column with different superscript letters differ significantly ($p < 0.05$). *These samples were not included in statistical analysis.

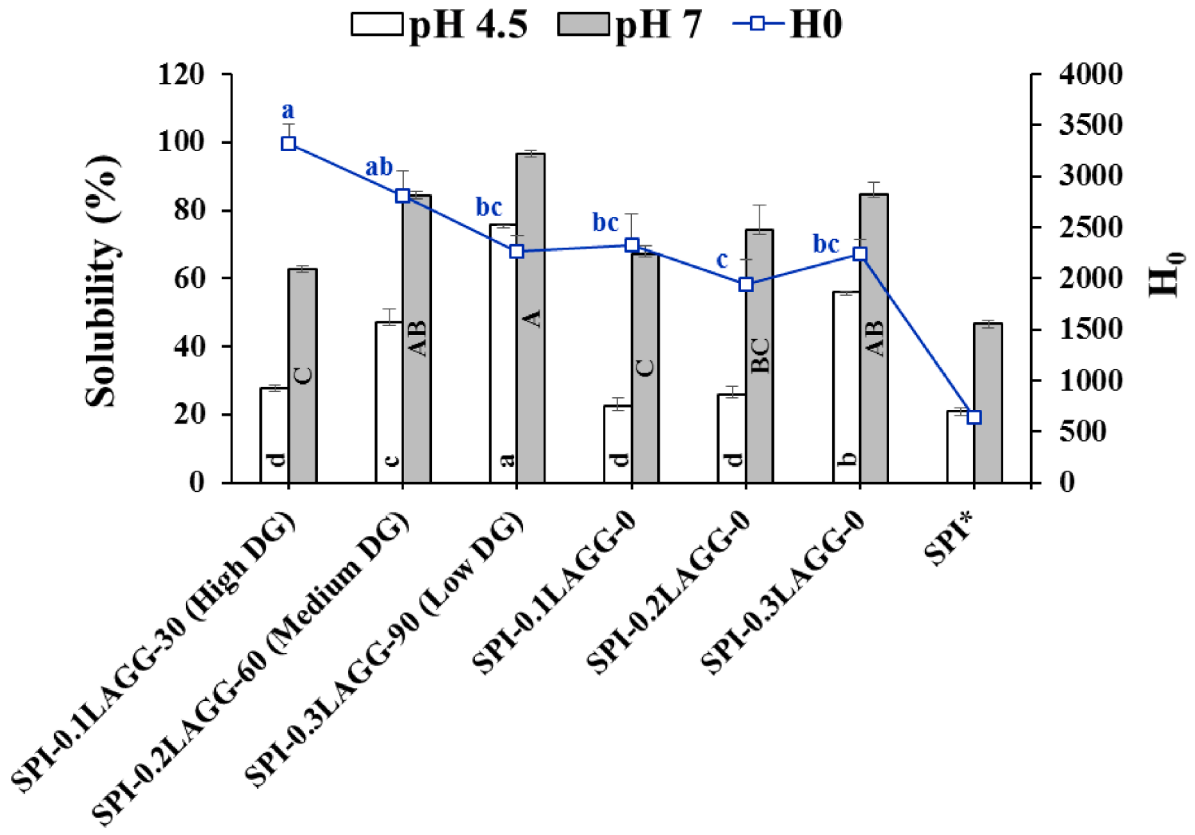

Fig. 3. Surface hydrophobicity and solubility (pH 4.5 and 7) and of soy protein isolate (SPI) and soy protein isolate-low acyl gellan gum (SPI-LAGG) mixtures and conjugates. *The sample designated SPI was not included in statistical analysis.

fold) compared to other pairs in the reaction medium (Wang et al., 2014). It is also noteworthy that all the SPI-LAGG mixture (up to about 3.9-fold) and SPI-LAGG conjugate systems (up to about 5-fold) had higher H_0 values than unheated SPI, suggesting that more hydrophobic regions were exposed to the environment to react with ANS (Wang et al., 2019).

3.4. Technofunctional properties

3.4.1. Solubility

The solubility of SPI, SPI-LAGG-0, and SPI-LAGG conjugates at pH 7 and near to isoelectric point (pI ~ 4.5) are provided in Fig. 3. The systems experienced a solubility increase as a function of conjugation and LAGG concentration ($p < 0.05$). Conjugation of SPI-LAGG mixtures led to an increase in the solubility on average from 75.42% to 81.32% at neutral conditions. The Maillard glycation is able to reduce protein aggregation and, in turn, increase its solubility through increasing protein-solvent interactions and lowering protein–protein interactions (Nooshkam et al., 2020). In addition, the anionic nature of the polysaccharide moiety could lead to a further increase in solubility by providing electrostatic repulsion between protein molecules as well as hydration shells around ionic groups (Ma, Chen, et al., 2020). In addition, it should be noted that both SPI and LAGG had a strong negative charge under reaction conditions (pH = 7), and electrostatic repulsive interactions between biopolymers could be increased as a result of LAGG content increment, thereby leading to a higher protein solubility (Nooshkam & Varidi, 2020b).

The SPI-LAGG conjugate with low DG had higher solubility than other conjugates (up to approximately 1.54-fold). Indeed, comparisons between conjugates show that higher DG doesn't necessarily lead to higher protein solubility (Álvarez et al., 2012). More covalent attachment of HMW LAGG to SPI has resulted in the formation of heavier conjugates (i.e., SPI-0.1LAGG-30 system; high DG) than other pairs, which could increase the probability of protein sedimentation during the essay. In addition, the higher H_0 value of SPI-0.1LAGG-30 system compared to other systems could justify its lower solubility (Fig. 3) (Nooshkam et al., 2020).

The protein solubility at its isoelectric point (pI ~ 4.5) showed a similar behavior (Fig. 3). Conjugation of SPI-LAGG physical mixtures also resulted in a remarkable solubility increase on average from 34.81% to 50.23% ($p < 0.05$). Proteins solubility improvement at the pI could be due to protein aggregation-inhibition *via* steric repulsions triggered by the LAGG moiety (Zhao et al., 2020), and the capability of the Maillard conjugation to shift the proteins' pI towards more acidic pHs (Nooshkam & Madadlou, 2016b). Note also that the DG exhibited a marked effect on the conjugates' solubility; the low DG provided a conjugate with greater solubility (up to 2.73-fold) compared to the other pairs. It is also noteworthy that the native SPI had poor solubility in both pH studied (46.63% and 20.95% at pH 7 and 4.5, respectively).

3.4.2. Viscosity

All SPI-LAGG systems indicated a shear thinning behavior (non-Newtonian pseudoplastic fluid) with a flow index of $n < 1$ ($n = 0.5$–0.86) (Table 2). The K and η_{50} values of SPI-LAGG mixture systems remarkably decreased after conjugation ($p < 0.05$). The conjugation reaction is able to lower gellan-gellan and protein–protein interactions and increase protein-gellan ones (Nooshkam & Varidi, 2021). It is generally agreed that at high temperatures, gellan gum polysaccharide forms random coils in solution with a low viscosity, and decreasing the temperature allows the gellan to cross-link through formation of double helices; so, gellan gum's viscosity increases dramatically to form a gel (Pastuszka & MacKay, 2016). On this point, the Maillard reaction between SPI and LAGG could reduce the gellan-gellan interactions and in turn double helices formation, leading to a lower viscosity.

Table 2
Rheological, oil/water interfacial, and air/water interfacial properties of soy protein isolate (SPI) and soy protein isolate-low acyl gellan gum (SPI-LAGG) mixtures and conjugates.

Parameters	Samples						
	SPI-0.1LAGG-30 (High DG)	SPI-0.2LAGG-60 (Medium DG)	SPI-0.3LAGG-90 (Low DG)	SPI-0.1LAGG-0	SPI-0.2LAGG-0	SPI-0.3LAGG-0	SPI*
Rheological properties							
K (Pa s^n)	0.032 ± 0.003^{d}	0.047 ± 0.002^{cd}	0.164 ± 0.002^{b}	0.033 ± 0.002^{d}	0.065 ± 0.013^{c}	0.247 ± 0.010^{a}	0.001 ± 0.000
n	0.86 ± 0.03^{a}	0.69 ± 0.01^{b}	0.56 ± 0.00^{cd}	0.82 ± 0.06^{a}	0.65 ± 0.04^{bc}	0.50 ± 0.01^{d}	1.04 ± 0.10
R^2	0.999	0.998	0.998	0.999	0.998	0.996	0.998
η_{50} (cP)	21.56 ± 0.27^{e}	53.99 ± 0.54^{d}	112.19 ± 2.43^{b}	18.28 ± 1.27^{e}	64.20 ± 1.75^{c}	137.66 ± 0.68^{a}	5.08 ± 0.00
Oil/water interfacial activity							
Interfacial tension (mN m^{-1})	5.15 ± 0.21^{b}	4.92 ± 0.19^{b}	3.69 ± 0.00^{a}	5.74 ± 0.27^{b}	5.64 ± 0.34^{b}	5.44 ± 0.07^{b}	5.93 ± 0.14
EAI (m^2 g^{-1})	2.325 ± 0.004^{c}	2.496 ± 0.004^{c}	4.068 ± 0.002^{a}	1.934 ± 0.020^{d}	2.501 ± 0.002^{c}	3.429 ± 0.139^{b}	0.943 ± 0.002
ESI (min)	54.078 ± 0.010^{c}	75.721 ± 0.034^{b}	122.659 ± 2.471^{a}	32.924 ± 0.032^{d}	49.625 ± 0.099^{c}	78.955 ± 4.508^{b}	39.849 ± 0.030
Droplet size (μm)	0.636 ± 0.005^{c}	0.596 ± 0.035^{c}	0.523 ± 0.003^{d}	1.047 ± 0.014^{a}	1.037 ± 0.018^{a}	0.864 ± 0.010^{b}	1.077 ± 0.023
PDI	0.14 ± 0.01^{c}	0.29 ± 0.03^{c}	0.24 ± 0.01^{c}	2.08 ± 0.15^{a}	1.77 ± 0.46^{ab}	1.18 ± 0.12^{b}	1.86 ± 0.21
ζ-potential (mV)	-20.57 ± 0.31^{a}	-22.77 ± 0.63^{a}	-26.09 ± 1.26^{b}	-29.33 ± 0.63^{c}	-31.42 ± 0.00^{cd}	-33.20 ± 1.05^{d}	-17.68 ± 1.10
Air/water interfacial activity							
Surface tension (mN m^{-1})	44.24 ± 0.11^{e}	44.53 ± 0.13^{de}	46.69 ± 0.08^{b}	44.76 ± 0.09^{cd}	45.11 ± 0.13^{c}	47.94 ± 0.10^{a}	43.62 ± 0.08
FC (%)	19.80 ± 1.47^{a}	14.14 ± 0.20^{b}	10.00 ± 0.00^{c}	7.34 ± 0.10^{d}	7.37 ± 0.05^{d}	3.68 ± 0.25^{e}	23.50 ± 2.12
FS (%)	73.95 ± 5.49^{b}	100.00 ± 0.00^{a}	100.00 ± 0.00^{a}	62.70 ± 4.43^{b}	93.78 ± 8.79^{a}	100.00 ± 0.00^{a}	62.75 ± 2.23

Means within the same row with different superscript letters differ significantly ($p < 0.05$).
*The sample designated SPI was not included in statistical analysis.

There was a significant difference ($p < 0.05$) in the K and η_{50} values of conjugates with low, medium, and high DG; K and η_{50} were decreased as the glycation degree increased. SPI-0.3LAGG-90 conjugate solution (low DG) had lower n and higher K values compared to other conjugates. The Maillard reaction progression and the formation of HMW compounds resisting against the flow could be higher in SPI-0.3LAGG-90 conjugate in comparison with other conjugates, leading to a marked increase in viscosity than other pairs (Nooshkam & Madadlou, 2016b).

3.4.3. Oil/water interfacial activity

The conjugate provided a significantly lower interfacial tension compared to the non-heated counterpart (4.58 *vs* 5.61 mN m^{-1}) (Table 2). Note also that the interfacial tension reduced markedly as a function of gellan level in the systems ($p < 0.05$). Accordingly, the conjugation reaction led to a significant increase in the EAI of SPI-LAGG mixture systems, on average from 2.621 m^2g^{-1} to 2.963 m^2g^{-1} (Table 2). Indeed, SPI-LAGG conjugates-stabilized emulsions had significantly lower particle size along with more homogenous and narrow particle size distribution (PDI) than those stabilized using physical mixtures and protein. SPI-0.3LAGG-90 conjugate had an improved emulsifying properties in comparison to other counterparts, indicating higher EAI (up to 4.314-fold) than the native SPI. In general, protein glycation improves emulsion formation capacity mainly due to increase in protein solubility, modifying H_0, and obtaining a more tuned hydrophile-lipophile balance (Nooshkam & Madadlou, 2016b). The H_0 increment after conjugation reaction (Fig. 3) may trigger hydrophobic interactions between oil droplets and interfacial protein, which facilitates protein molecules attachment to the oil droplets' surface and reduces interfacial tension greatly (Nooshkam & Varidi, 2020b). In fact, structural changes in glycated protein could lead to the formation of flexible structures with faster migration, adsorption, and rearrangement processes to oil/water interface (Li et al., 2019). On the other hand, the EAI of the SPI-LAGG physical mixtures significantly enhanced ($p < 0.05$) as the concentration of LAGG increased; 0.3%LAGG and 0.1% LAGG systems displayed the highest and lowest EAI, respectively (Table 2). This could be likely due to the presence of a few protein moieties and the hydrophobicity of the acyl groups in the LAGG structure (Fasolin et al., 2013).

There was a notable difference in the EAI of the conjugates. The DG increase led to a marked decrease in the EAI on average from 4.068 m^2/g (low DG) to 2.325 m^2g^{-1} (high DG), demonstrating an up to 1.75-fold higher EAI in the low DG compared to the medium and high DG clusters. These results were in agreement with findings of Li et al. (2013), who reported that the binding site of the protein at oil/water interface is reduced as a result of DG increment, and the optimal hydrophilic-lipophilic balance is required for interfacial adsorption.

The ESI of SPI-LAGG mixture systems remarkably increased after conjugation (53.81–84.15 min), which was confirmed by the results of particle size test (Table 2). Moreover, the emulsions stabilized by the SPI-LAGG conjugates had higher stability (up to about 2-fold) than SPI-stabilized one. This is mainly due to the high ability of conjugates to form a thicker, cohesive, and viscoelastic interfacial layer at the oil/water interface (Kutzli et al., 2021). The protein moiety anchors on the surface of hydrophobic parts, and the polysaccharide moiety prevents oil droplets aggregations due to self-assembled networks formation at the interface and electro-steric repulsion (Nooshkam & Varidi, 2021). Also, the ESI increased markedly as the concentration of LAGG increased; 0.3%LAGG and 0.1%LAGG-based systems had the highest and lowest ESI, respectively. LAGG, through thickening effect and increasing the viscosity of continuous phase, leads to retardation of Brownian motion of the droplets and in turn droplet collision frequency, so emulsion stability improves (O'Regan & Mulvihill, 2010). In addition, ζ-potential increment of emulsions stabilized by SPI-LAGG pairs as a function of LAGG content could be another explanation for this behavior

(Table 2).

As can be observed in Table 2, the ESI decreased remarkably as the DG increased. SPI-0.3LAGG-90 and SPI-0.1LAGG-30 conjugates showed the highest and lowest ESI, respectively; the low DG conjugate had an up to 2.27-fold higher ESI than other conjugates. This could be likely due to the more presence of free polysaccharides (non-absorbing polysaccharides) in the continuous phase of SPI-0.3LAGG-90 emulsion than other counterparts (O'Regan & Mulvihill, 2010). It is also noteworthy that the emulsion prepared with SPI exhibited a weak EAI and ESI with the highest droplet sizes, as expected.

The emulsions stabilized by SPI-LAGG conjugates had significantly lower negative ζ-potential (–23.14 mV) compared to those stabilized by the mixtures (-31.31 mV) ($p < 0.05$). This might be likely attributed to the fact that the bound LAGG molecules could have a substantial effect on the distance from the droplet surfaces where the effective electrical properties are measured (i.e., the shear plane). In fact, the presence of bound LAGG molecules leads to electrical charge determination at a distances further from the surface of droplets; therefore, causes a greater decrease in the electrical potential (Nooshkam & Varidi, 2021).

3.4.4. Air/water interfacial activity

The conjugates generally lowered the surface tension more efficiently in comparison to the non-conjugated pairs ($p < 0.05$) (Table 2). Moreover, the lower the gellan content, the lower was the surface tension ($p < 0.05$). The FC and FS of native SPI, SPI-LAGG mixtures, and their conjugates were consequently influenced by the surface tension changes. It was clear that FC of SPI-LAGG physical mixtures substantially increased from 6.13% to 14.65% after conjugation reaction ($p < 0.05$) as a result of modifying hydrophile-lipophile balance, while FS did not change significantly after glycation ($p > 0.05$). Moreover, the high H_0, flexibility, and surface activity might lead to an increase in the FC of proteins (Li et al., 2019). The LAGG content had a significant adverse effect on the FC of the systems ($p < 0.05$). As a matter of fact, the FC decreased markedly as the LAGG level increased. Accordingly, SPI-0.1LAGG system showed significantly higher FC (13.57%) compared to the SPI-0.2LAGG and SPI-0.3LAGG systems (10.76% and 6.84%, respectively) ($p < 0.05$). The decrease in protein's FC might be mainly due to the structural changes, high viscosity, and decreased H_0 of protein as a result of LAGG level increment (Fig. 3). It is noteworthy that a marked decrease in FC of SPI solution from 23.50% to 3.68% (i.e., SPI-0.3LAGG mixture) was observed in the presence of LAGG. As shown in Table 2, the high DG displayed superior FC in comparison with medium DG and low DG conjugates, which was consistent with the surface tension observations.

The FS was remarkably increased with rising LAGG content in the system ($p < 0.05$). Accordingly, maximum and minimum FS were accounted for the systems containing 0.3% (100%) and 0.1% (68.32%) LAGG content, respectively (Table 2). Moreover, when LAGG was added into the system, the FS of SPI solution (65.75%) was increased up to 100%. This could be ascribed to the improved viscosity and steric/electrostatic repulsive forces due to the presence of LAGG, delaying the aggregation and coalescence between bubbles. Moreover, the LAGG and conjugates have a potential to form a self-assembled network and bulkier polymeric layer at the air/water interface to stabilize the foam structure (Nooshkam & Varidi, 2020b). According to Table 2, it can be seen that although systems with low and medium DG showed an equal amount of the FS (100%) ($p > 0.05$), this parameter decreased significantly (73.95%) ($p < 0.05$) in the system with high DG due to its lower solubility and viscosity.

3.5. Antioxidant activity

It was clear that the unheated SPI solution had a poor antioxidant capacity (Fig. 4). In general, the presence of reducing sugars in the reaction medium led to a substantial increase in the antioxidant activity of all systems including SPI-LAGG pairs. Accordingly, 0.3%LAGG and 0.1% LAGG-based systems presented the highest and lowest antioxidant activity, respectively. However, the antioxidant activity of SPI-LAGG physical mixtures decreased remarkably after conjugation reaction, likely due to MRPs' degradation or complexity (Nooshkam, Varidi, et al., 2019). The antioxidant properties of the systems decreased markedly as the DG increased. The high DG, medium DG, and low DG systems had

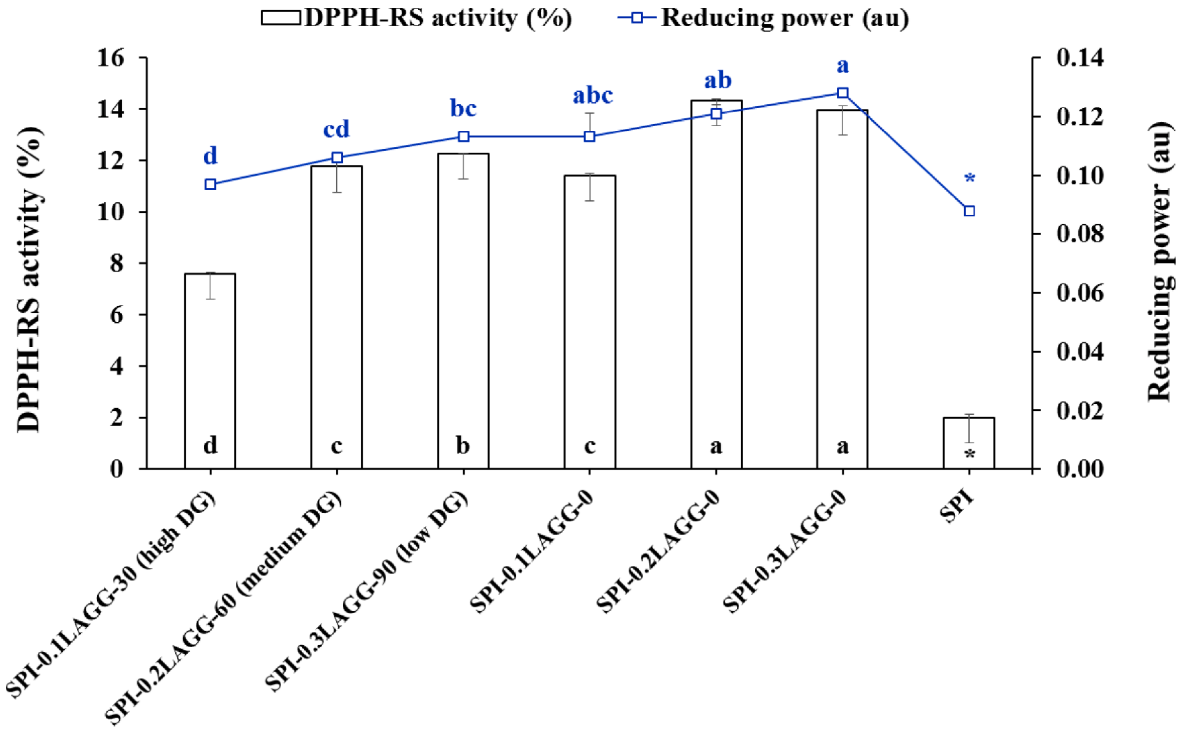

Fig. 4. Antioxidant activity of soy protein isolate (SPI) and soy protein isolate-low acyl gellan gum (SPI-LAGG) mixtures and conjugates. *The sample designated SPI was not included in statistical analysis.

33.45%, 17.92%, and 12.23% DPPH-RS activity compared to the corresponding physical mixtures, respectively. However, the reducing power decreased with less intensity. Antioxidant activity of conjugates is mainly due to the intermediate products and melanoidins (Nooshkam et al., 2020).

4. Conclusions

The effect of DG on the structural changes and technological functionality of SPI-LAGG conjugates was evaluated in the present study. The high DG led to conjugates with poor techno-functional properties (except for foaming capacity) compared to those with medium and low DG. Nonetheless, the low DG-based SPI-LAGG conjugates indicated improved functional properties, particularly solubility and emulsion formation/stability. The results demonstrated that a low DG is needed to improve the functional characteristics of SPI and its industrial applications. Indeed, this study confirmed the hypothesis that the classification of Maillard reaction-based protein-polysaccharide conjugates through *K*-means clustering could help predict their technological functionality and biological properties as the first step in their use as food ingredients. The SPI-LAGG conjugates with low DG (SPI-0.3LAGG-90) have therefore remarkable potential for use as food-grade functional ingredients for the development of highly stable colloidal food systems. However, the fate of SPI-LAGG conjugate-stabilized colloidal systems under environmental conditions such as pH, temperature, salt, and freeze–thaw treatments need to be evaluated in future works.

CRediT authorship contribution statement

Yasaman Lavaei: Methodology, Investigation, Resources, Software, Writing – original draft. **Mehdi Varidi:** Supervision, Funding acquisition, Conceptualization, Methodology, Visualization, Validation, Writing – review & editing. **Majid Nooshkam:** Methodology, Visualization, Validation, Software, Writing – review & editing.

Declaration of Competing Interest

The authors declare that they have no known competing financial interests or personal relationships that could have appeared to influence the work reported in this paper.

Acknowledgment

The authors thank Ferdowsi University of Mashhad (Mashhad, Iran) for financial support of this project (Grant No. 3/52971).

References

Abellán, G., Coronado, E., Gómez-García, C. J., Martí-Gastaldo, C., & Ribera, A. (2013). Intercalation of cobalt(II)-tetraphenylporphine tetrasulfonate complex in magnetic NiFe-layered double hydroxide. *Polyhedron, 52*, 216–221. https://doi.org/10.1016/j.poly.2012.09.045

Álvarez, C., García, V., Rendueles, M., & Díaz, M. (2012). Functional properties of isolated porcine blood proteins modified by Maillard's reaction. *Food Hydrocolloids, 28*(2), 267–274. https://doi.org/10.1016/j.foodhyd.2012.01.001

Boostani, S., Aminlari, M., Moosavi-nasab, M., Niakosari, M., & Mesbahi, G. (2017). Fabrication and characterisation of soy protein isolate-grafted dextran biopolymer: A novel ingredient in spray-dried soy beverage formulation. *International Journal of Biological Macromolecules, 102*, 297–307. https://doi.org/10.1016/j.ijbiomac.2017.04.019

Caballero, S., & Davidov-Pardo, G. (2021). Comparison of legume and dairy proteins for the impact of Maillard conjugation on nanoemulsion formation, stability, and lutein color retention. *Food Chemistry, 338*, Article 128083. https://doi.org/10.1016/j.foodchem.2020.128083

Chen, B., Cai, Y., Liu, T., Huang, L., Zhao, X., Zhao, M., … Zhao, Q. (2020). Formation and performance of high acyl gellan hydrogel affected by the addition of physical-chemical treated insoluble soybean fiber. *Food Hydrocolloids, 101*, Article 105526. https://doi.org/10.1016/j.foodhyd.2019.105526

Consoli, L., Dias, R. A. O., Rabelo, R. S., Furtado, G. F., Sussulini, A., Cunha, R. L., & Hubinger, M. D. (2018). Sodium caseinate-corn starch hydrolysates conjugates obtained through the Maillard reaction as stabilizing agents in resveratrol-loaded emulsions. *Food Hydrocolloids, 84*, 458–472. https://doi.org/10.1016/j.foodhyd.2018.06.017

Damodaran, S., & Parkin, K. L. (2017). Amino acids, peptides, and proteins. In *Fennema's food chemistry* (pp. 235–356). CRC Press.

Denavi, G., Tapia-Blácido, D. R., Añón, M. C., Sobral, P. J. A., Mauri, A. N., & Menegalli, F. C. (2009). Effects of drying conditions on some physical properties of soy protein films. *Journal of Food Engineering, 90*(3), 341–349. https://doi.org/10.1016/j.jfoodeng.2008.07.001

Fasolin, L. H., Picone, C. S. F., Santana, R. C., & Cunha, R. L. (2013). Production of hybrid gels from polysorbate and gellan gum. *Food Research International, 54*(1), 501–507. https://doi.org/10.1016/j.foodres.2013.07.026

Feyzi, S., Varidi, M., Zare, F., & Varidi, M. J. (2018). Effect of drying methods on the structure, thermo and functional properties of fenugreek (Trigonella foenum graecum) protein isolate. *Journal of the Science of Food and Agriculture, 98*(5), 1880–1888. https://doi.org/10.1002/jsfa.8669

Kazemi-Taskooh, Z., & Varidi, M. (2021). Designation and characterization of cold-set whey protein-gellan gum hydrogel for iron entrapment. *Food Hydrocolloids, 111*, Article 106205. https://doi.org/10.1016/j.foodhyd.2020.106205

Kutzli, I., Weiss, J., & Gibis, M. (2021). Glycation of Plant Proteins Via Maillard Reaction: Reaction Chemistry, Technofunctional Properties, and Potential Food Application. *Foods, 10*(2). https://doi.org/10.3390/foods10020376

Lertittikul, W., Benjakul, S., & Tanaka, M. (2007). Characteristics and antioxidative activity of Maillard reaction products from a porcine plasma protein–glucose model system as influenced by pH. *Food Chemistry, 100*(2), 669–677. https://doi.org/10.1016/j.foodchem.2005.09.085

Li, R., Wang, X., Liu, J., Cui, Q., Wang, X., Chen, S., & Jiang, L. (2019). Relationship between Molecular Flexibility and Emulsifying Properties of Soy Protein Isolate-Glucose Conjugates. *Journal of Agricultural and Food Chemistry, 67*(14), 4089–4097. https://doi.org/10.1021/acs.jafc.8b06713

Li, Y., Zhong, F., Ji, W., Yokoyama, W., Shoemaker, C. F., Zhu, S., & Xia, W. (2013). Functional properties of Maillard reaction products of rice protein hydrolysates with mono-, oligo- and polysaccharides. *Food Hydrocolloids, 30*(1), 53–60. https://doi.org/10.1016/j.foodhyd.2012.04.013

Ma, X., Chen, W., Yan, T., Wang, D., Hou, F., Miao, S., & Liu, D. (2020). Comparison of citrus pectin and apple pectin in conjugation with soy protein isolate (SPI) under controlled dry-heating conditions. *Food Chemistry, 309*, Article 125501. https://doi.org/10.1016/j.foodchem.2019.125501

Ma, X., Hou, F., Zhao, H., Wang, D., Chen, W., Miao, S., & Liu, D. (2020). Conjugation of soy protein isolate (SPI) with pectin by ultrasound treatment. *Food Hydrocolloids, 108*, Article 106056. https://doi.org/10.1016/j.foodhyd.2020.106056

Mao, L., Pan, Q., Hou, Z., Yuan, F., & Gao, Y. (2018). Development of soy protein isolate-carrageenan conjugates through Maillard reaction for the microencapsulation of Bifidobacterium longum. *Food Hydrocolloids, 84*, 489–497. https://doi.org/10.1016/j.foodhyd.2018.06.037

Martinez-Alvarenga, M. S., Martinez-Rodriguez, E. Y., Garcia-Amezquita, L. E., Olivas, G. I., Zamudio-Flores, P. B., Acosta-Muniz, C. H., & Sepulveda, D. R. (2014). Effect of Maillard reaction conditions on the degree of glycation and functional properties of whey protein isolate – Maltodextrin conjugates. *Food Hydrocolloids, 38*, 110–118. https://doi.org/10.1016/j.foodhyd.2013.11.006

Mozafarpour, R., Koocheki, A., Milani, E., & Varidi, M. (2019). Extruded soy protein as a novel emulsifier: Structure, interfacial activity and emulsifying property. *Food Hydrocolloids, 93*, 361–373. https://doi.org/10.1016/j.foodhyd.2019.02.036

Naik, R. R., Wang, Y., & Selomulya, C. (2021). Improvements of plant protein functionalities by Maillard conjugation and Maillard reaction products. *Critical Reviews in Food Science and Nutrition, 1–26*. https://doi.org/10.1080/10408398.2021.1910139

Namli, S., Sumnu, S. G., & Oztop, M. H. (2021). Microwave glycation of soy protein isolate with rare sugar (D-allulose), fructose and glucose. *Food Bioscience, 40*, Article 100897. https://doi.org/10.1016/j.fbio.2021.100897

Nasrollahzadeh, F., Varidi, M., Koocheki, A., & Hadizadeh, F. (2017). Effect of microwave and conventional heating on structural, functional and antioxidant properties of bovine serum albumin-maltodextrin conjugates through Maillard reaction. *Food Research International, 100*, 289–297. https://doi.org/10.1016/j.foodres.2017.08.030

Nooshkam, M., Falah, F., Zareie, Z., Tabatabaei Yazdi, F., Shahidi, F., & Mortazavi, S. A. (2019). Antioxidant potential and antimicrobial activity of chitosan–inulin conjugates obtained through the Maillard reaction. *Food Science and Biotechnology, 28*(6), 1861–1869. https://doi.org/10.1007/s10068-019-00635-3

Nooshkam, M., & Madadlou, A. (2016a). Maillard conjugation of lactulose with potentially bioactive peptides. *Food Chemistry, 192*, 831–836. https://doi.org/10.1016/j.foodchem.2015.07.094

Nooshkam, M., & Madadlou, A. (2016b). Microwave-assisted isomerisation of lactose to lactulose and Maillard conjugation of lactulose and lactose with whey proteins and peptides. *Food Chemistry, 200*, 1–9. https://doi.org/10.1016/j.foodchem.2015.12.094

Nooshkam, M., & Varidi, M. (2020a). Maillard conjugate-based delivery systems for the encapsulation, protection, and controlled release of nutraceuticals and food bioactive ingredients: A review. *Food Hydrocolloids, 100*, Article 105389. https://doi.org/10.1016/j.foodhyd.2019.105389

Nooshkam, M., & Varidi, M. (2020b). Whey protein isolate-low acyl gellan gum Maillard-based conjugates with tailored technological functionality and antioxidant activity. *International Dairy Journal, 109*, Article 104783. https://doi.org/10.1016/j.idairyj.2020.104783

Nooshkam, M., & Varidi, M. (2021). Physicochemical stability and gastrointestinal fate of β-carotene-loaded oil-in-water emulsions stabilized by whey protein isolate-low acyl

gellan gum conjugates. *Food Chemistry, 347*, Article 129079. https://doi.org/10.1016/j.foodchem.2021.129079

Nooshkam, M., Varidi, M., & Bashash, M. (2019). The Maillard reaction products as food-born antioxidant and antibrowning agents in model and real food systems. *Food Chemistry, 275*, 644–660. https://doi.org/10.1016/j.foodchem.2018.09.083

Nooshkam, M., Varidi, M., & Verma, D. K. (2020). Functional and biological properties of Maillard conjugates and their potential application in medical and food: A review. *Food Research International, 131*, Article 109003. https://doi.org/10.1016/j.foodres.2020.109003

O'Regan, J., & Mulvihill, D. M. (2010). Heat stability and freeze–thaw stability of oil-in-water emulsions stabilised by sodium caseinate–maltodextrin conjugates. *Food Chemistry, 119*(1), 182–190. https://doi.org/10.1016/j.foodchem.2009.06.019

Pastuszka, M. K., & MacKay, J. A. (2016). Engineering structure and function using thermoresponsive biopolymers. *WIREs Nanomedicine and Nanobiotechnology, 8*(1), 123–138. https://doi.org/10.1002/wnan.1350

Pearce, K. N., & Kinsella, J. E. (1978). Emulsifying properties of proteins: Evaluation of a turbidimetric technique. *Journal of Agricultural and Food Chemistry, 26*(3), 716–723. https://doi.org/10.1021/jf60217a041

Petruccelli, S., & Anon, M. C. (1995). Soy Protein Isolate Components and Their Interactions. *Journal of Agricultural and Food Chemistry, 43*(7), 1762–1767. https://doi.org/10.1021/jf00055a004

Su, J.-F., Huang, Z., Yuan, X.-Y., Wang, X.-Y., & Li, M. (2010). Structure and properties of carboxymethyl cellulose/soy protein isolate blend edible films crosslinked by Maillard reactions. *Carbohydrate Polymers, 79*(1), 145–153. https://doi.org/10.1016/j.carbpol.2009.07.035

Uruakpa, F. O., & Arntfield, S. D. (2006). Surface hydrophobicity of commercial canola proteins mixed with κ-carrageenan or guar gum. *Food Chemistry, 95*(2), 255–263. https://doi.org/10.1016/j.foodchem.2005.01.030

Wang, Y., Gan, J., Li, Y., Nirasawa, S., & Cheng, Y. (2019). Conformation and emulsifying properties of deamidated wheat gluten-maltodextrin/citrus pectin conjugates and their abilities to stabilize β-carotene emulsions. *Food Hydrocolloids, 87*, 129–141. https://doi.org/10.1016/j.foodhyd.2018.07.050

Wang, Z., Li, Y., Jiang, L., Qi, B., & Zhou, L. (2014). Relationship between Secondary Structure and Surface Hydrophobicity of Soybean Protein Isolate Subjected to Heat Treatment. *Journal of Chemistry, 2014*, Article 475389. https://doi.org/10.1155/2014/475389

Zhao, C., Yin, H., Yan, J., Qi, B., & Liu, J. (2020). Structural and physicochemical properties of soya bean protein isolate/maltodextrin mixture and glycosylation conjugates. *International Journal of Food Science & Technology, 55*(10), 3315–3326. https://doi.org/10.1111/ijfs.14595